DALTON
FULL PAPER

Encapsulated Tl(III) strongly retained within an iminophenolate cryptand host

Michael G. B. Drew,[a] Oliver W. Howarth,[b] Noreen Martin,[c,d] Grace G. Morgan[c,d] and Jane Nelson[c,d]

[a] *Chemistry Department, The University, Reading, UK RG2 6AD*
[b] *Department of Chemistry, University of Warwick, Coventry, UK CV4 7AL*
[c] *School of Chemistry, Queens University, Belfast, UK BT9 5AG*
[d] *Open University, Milton Keynes, UK MK7 6AA*

Received 27th January 2000, Accepted 2nd March 2000
Published on the Web 30th March 2000

The crystal structure of a thallium(III) iminophenolate cryptate is reported. Tl(III) is strongly held within the host, as judged by NMR indicators of strength of binding, by both imino-N, (*via* ^{203,205}Tl,^{15}N coupling of over 1000 Hz in the MAS-CP spectrum) and phenolate-O donors (*via* the weakness of competitive H-bonding to the phenolate O^- groups, seen in the solution ^{1}H spectrum).

While thallium isotopes such as ^{201}Tl have desirable nuclear properties for some applications, *e.g.* heart imaging,[1] and as a putative therapeutic treatment against tumours,[2] there has been some resistance to biomedical use of the element on account of the considerable toxicity of free Tl^+(aq). Any host with efficient kinetic and thermodynamic resistance to decomplexation is thus of interest as it may find use in thallotoxicosis treatment. Both the imaging application and the toxicity arise from the fact that the free aqueous +1 redox state cation mimics potassium,[3] ensuring that the radioisotope is carried to sites of important biological function. For detoxification and therapeutic purposes, it may be preferable to handle the element in its +3 redox state, since it no longer mimics potassium in this form and is more strongly coordinated, particularly by anionic donors. Both thermodynamic and kinetic stabilization are associated with the cryptate effect, as is well documented,[4] hence an anionic cryptand host capable of stabilising the +3 redox state of thallium has a two-fold chance of producing the desired reduction in toxicity, as even after any *in vivo* reduction, the +1 cation will still, to some extent, be kinetically stabilised within the cryptand host.

Results and discussion

Treatment of the monosodium salt of the phenolate cryptand host L^1 with Tl^{3+} results in generation of the monothallic cryptate $[TlL^1](ClO_4)_3$, **1**. There is unambiguous NMR evidence (*q.v.*) that the phenol OH groups have been deprotonated, with proton transfer to the uncoordinated imine functions, a strategy adopted[5] by other cryptates of this ligand. On recrystallisation from acetonitrile–ethanol, small yellow cubes of **1** suitable for X-ray crystallography were obtained.

The structure contains $[TlL^1]^{3+}$ cations and uncoordinated

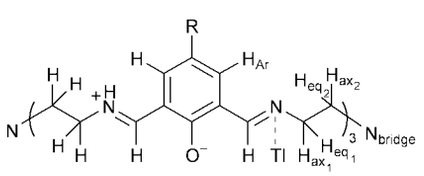

L^1, R = CH_3; L^2, R = ^{t}Bu
One of three identical strands of L^1 is shown

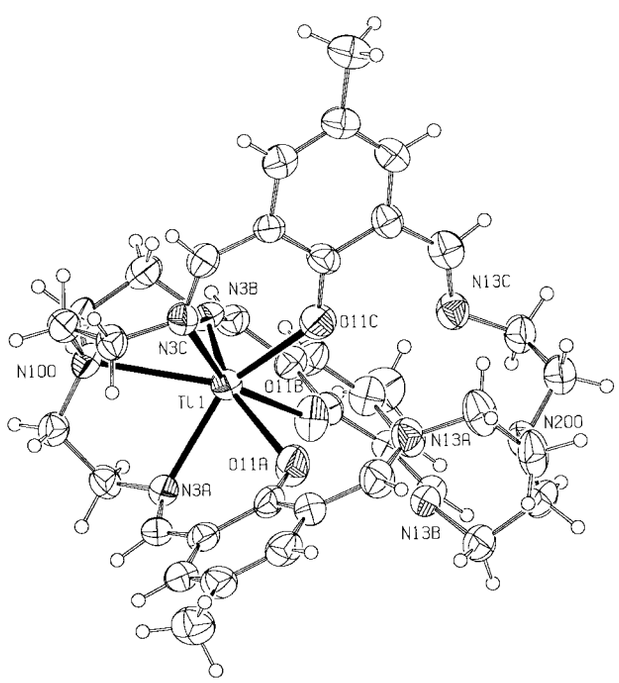

Fig. 1 Structure of **1**. The major component of the disorder is shown. Selected distances (Å): Tl–N_{bridge} 2.689(7); Tl–N_{im} 2.339(8), 2.346(8), 2.369(8); Tl–O_{OPh} 2.230(7), 2.234(7), 2.287(7).

ClO_4^- anions, and the cation is disordered over two positions (lying at opposite ends of the cryptand host) with relative occupancies of 0.59(1) and 0.41(1); the major component is shown in Fig. 1. Distances around both positions of the metal are listed in Table 1 and show very little difference between the two coordination spheres. The thallium cation sits unsymmetrically in the cryptand cavity, so that one end of the potentially binucleating ligand contains the tripositive cation and the other the three transferred protons. Tl(III) is seven coordinate in both positions, with a geometry which may be described as capped octahedral, and, as expected from the relatively higher charge density on the cation, forms shorter M–O and M–N_{imine} contacts than the Pb(II) analogue reported previously.[5] It is perhaps surprising, that there is a particularly noticeable contraction in the M–N_{imino} distances in comparison with the Pb(II) cryptate,

DOI: 10.1039/b000736f

Table 1 Bond lengths (Å) and angles (°) for **1**

Tl(1)–O(11B)	2.230(7)	Tl(2)–O(11A)	2.178(7)
Tl(1)–O(11C)	2.234(7)	Tl(2)–O(11C)	2.234(7)
Tl(1)–O(11A)	2.287(7)	Tl(2)–O(11B)	2.261(7)
Tl(1)–N(3B)	2.339(8)	Tl(2)–N(13B)	2.335(8)
Tl(1)–N(3A)	2.346(8)	Tl(2)–N(13A)	2.386(9)
Tl(1)–N(3C)	2.369(8)	Tl(2)–N(13C)	2.414(9)
Tl(1)–N(100)	2.689(7)	Tl(2)–N(200)	2.653(9)
Tl(1)···Tl(2)	3.107(4)		
O(11B)–Tl(1)–O(11C)	78.5(3)	N(3A)–Tl(1)–N(3C)	106.9(3)
O(11B)–Tl(1)–O(11A)	74.0(3)	O(11B)–Tl(1)–N(100)	134.2(2)
O(11C)–Tl(1)–O(11A)	77.1(3)	O(11C)–Tl(1)–N(100)	134.9(2)
O(11B)–Tl(1)–N(3B)	75.9(3)	O(11A)–Tl(1)–N(100)	133.7(2)
O(11C)–Tl(1)–N(3B)	95.4(3)	N(3B)–Tl(1)–N(100)	71.4(3)
O(11A)–Tl(1)–N(3B)	149.9(3)	N(3A)–Tl(1)–N(100)	69.0(2)
O(11B)–Tl(1)–N(3A)	95.9(3)	N(3C)–Tl(1)–N(100)	69.2(2)
O(11C)–Tl(1)–N(3A)	149.7(3)	O(11A)–Tl(2)–O(11C)	79.4(3)
O(11A)–Tl(1)–N(3A)	72.8(3)	O(11A)–Tl(2)–O(11B)	75.5(3)
N(3B)–Tl(1)–N(3A)	112.2(3)	O(11C)–Tl(2)–O(11B)	77.8(3)
O(11B)–Tl(1)–N(3C)	153.1(3)	O(11A)–Tl(2)–N(13B)	100.1(3)
O(11C)–Tl(1)–N(3C)	74.6(3)	O(11C)–Tl(2)–N(13B)	147.9(3)
O(11A)–Tl(1)–N(3C)	98.9(3)	O(11B)–Tl(2)–N(13B)	71.1(3)
N(3B)–Tl(1)–N(3C)	107.2(3)	O(11A)–Tl(2)–N(13A)	73.2(3)
O(11C)–Tl(2)–N(13A)	94.3(3)	N(13A)–Tl(2)–N(13C)	105.7(3)
O(11B)–Tl(2)–N(13A)	148.7(3)	O(11A)–Tl(2)–N(200)	132.9(3)
N(13B)–Tl(2)–N(13A)	116.6(3)	O(11C)–Tl(2)–N(200)	133.6(3)
O(11A)–Tl(2)–N(13C)	150.9(3)	O(11B)–Tl(2)–N(200)	134.4(3)
O(11C)–Tl(2)–N(13C)	71.6(3)	N(13B)–Tl(2)–N(200)	69.3(3)
O(11B)–Tl(2)–N(13C)	100.4(3)	N(13A)–Tl(2)–N(200)	72.0(3)
N(13B)–Tl(2)–N(13C)	105.8(3)	N(13C)–Tl(2)–N(200)	70.3(3)

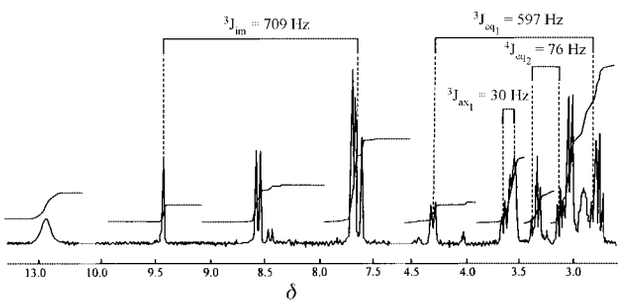

Fig. 2 400 MHz ^{1}H NMR spectrum of **1** in CD_3CN: chemical shifts in ppm from TMS, coupling constants (Hz) in parentheses. Major couplings to thallium indicated as $^nJ_{eq}$ (for equatorial methylene hydrogens) and $^nJ_{ax}$ (for axial methylene hydrogens) and $^3J_{im}$ (for imino hydrogens). NH^+ 12.94, s; CH_{im} 8.57, d (14.6), 8.54,[b] d (709.6); CH_{ar} 7.70, s, 7.63,[b] d (24.85); CH_2 2.76,[a] 3.03,[a] 3.56,[a] 3.07;[a] 3.56[a,b] (597), 3.60[a,b] (30), 3.24[a,b] (76), 2.89[a,b] (−10); CH_3.[c] [a] Proton–proton coupled, not assigned. [b] Coupling to ^{205,203}Tl in parentheses. [c] Overlapped, unassignable.

given that a more significant electrostatic effect between the tripositively charged cation and the phenolate donors might be anticipated. The Tl–O^- distances at 2.230(7), 2.234(7) and 2.287(7) Å are generally shorter than those recorded for coordination of Tl(III) by other anionic O donors (2.36, 2.46;[6] 2.29, 2.48[7] Å) while the Tl–N distances, at 2.339(8), 2.346(8) and 2.369(8) Å, are longer than seen in macrocyclic porphyrin or phthalocyanato[6–8] Tl(III) complexes where covalency in the Tl–N bond is reported (2.21–2.22 Å). The metal–ligand distances are similar to those in the analogous series of isomorphous lanthanoid cryptates characterised previously,[9] but, as expected, a good deal shorter than in similar Tl(I) complexes.[10,11]

Two facets of the solution ^{1}H NMR spectrum of **1** call for comment. One is the ^{1}H,^{203,205}Tl couplings, which are assigned on the basis of a 2-D COSY experiment; the larger couplings are labelled as ^3J and ^4J in Fig. 2. The magnitude of the three-bond coupling to the imino hydrogen is greatest, exceeding by *ca*. 100 Hz that for the pseudoequatorial methylene H_{eq_1} and by a factor of >20 that for the pseudoaxial methylene H_{ax_1}; in this latter case the CH bond is thus inferred to make a dihedral angle with Tl–N close to 90°. In cryptates of this[5] and related[12] ligands with the magnetically active nuclei ^{111,113}Cd and ^{199}Hg, the $M\cdots CH_{imino}$ coupling is invariably the largest M,H coupling observed; about 55–65% larger than that to the pseudo-equatorial methylene proton. However, the low magnetic moment of these nuclei means that coupling is not discernible beyond the three-bond stage, as it is with ^{205,203}Tl(III). Four-bond ^{1}H,^{203,205}Tl, coupling is clearly seen to the pseudo equatorial proton H_{eq_2} adjacent to N_{bridge}, which is much larger than to the axial proton H_{ax_2}; in addition the coupling to the axial proton is negative, as expected for four-bond ^{1}H,^{203,205}Tl coupling, while the equatorial coupling is relatively large and positive, suggesting a more dominant direct interaction with thallium. For all comparable methylene pairs, the chemical shifts rise at the Tl end of the cryptate, indicating a general deshielding effect induced by thallium on the chemical shifts of the ^{1}H resonance positions. The observation of 5-bond coupling to ^{203,205}Tl, at 24.85 Hz, restricted to the thallium-end aromatic resonance H_{eAr}, suggests that covalency-mediated coupling *via* the phenolate O^- is unimportant compared with that *via* the imino-N donor. Resonances at 12.94 and 8.57 ppm in the non-thallium end of the cryptate arise from the uncoordinated protonated NH^+=CH imino function, as shown by decoupling of the 8.57 ppm doublet on irradiation of the 12.94 ppm resonance. Both the breadth and chemical shift of the 12.94 ppm resonance show it to be involved in H-bonding with the phenolate O^-, which is the second observation warranting comment.

Table 2 NH^+ chemical shifts[a] and ^3J(HC=NH) couplings[b] for L^1 and L^2 cryptates

Cryptate (M^{n+})	$\delta(NH^+)$	^3J(HC=NH)[b]/Hz
2: $(NaL^1)^{+}$[c]	14.73	4.49
4: $(CdL^1)^{2+}$[d]	13.89	13.63
6: $(ZnL^1)^{2+}$	13.86	13.65
5: $(PbL^1)^{2+}$[d]	13.59	13.47
3: $(CaL^1)^{2+}$	13.53	14.08
8: $(BiL^1)^{3+}$[e]	13.19	14.01
1: $(TlL^1)^{3+}$	12.94	14.63
7: $(InL^1)^{3+}$[e]	12.68	14.62
9: $(NaL^2)^{+}$[e]	14.86	8.36
10: $(YL^2)^{3+}$[e]	12.59	15.10
11:[f] $(InL^2)^{3+}$	12.40	14.88
12: $(ScL^2)^{3+}$	12.30	15.20

[a] Shifts in ppm from TMS; CD_3CN solutions, 295 K, unless otherwise stated. [b] Coupling constants in Hz. [c] Broad, just resolved signal near coalescence. [d] Ref. 5. [e] 233 K spectrum. [f] Run in d^6-DMSO.

An analogous situation has previously been reported in main group mononuclear cryptates of this ligand,[5,9,13,14] where the smaller cation cryptates share with the Tl(III) analogue the sharply resolved room temperature solution ^{1}H NMR spectrum, which testifies to kinetic stabilisation against decomplexation. When results from these other studies are collated (Table 2), it can be seen that the stronger the H-bond from NH^+ to O^- in the series of L^1 and L^2 cryptates, the weaker the vicinal CH=NH^+ coupling across the imino bond. In common with other tripositive cations, Tl(III) appears to weaken the H-bond by its electrostatic effect on the O^- acceptor. As in cryptates of the similarly sized Y(III) and In(III) cations, **10** and **11**, the NH^+ resonance of **1** shows a chemical shift of less than 13 ppm and CH=NH^+ *trans* coupling greater than 14 Hz, in comparison with, for example, NaL^1 and NaL^2, **2** and **9**, where the strong intramolecular H-bonds adopted generate the largest chemical shifts (>14.7 ppm) and smallest CH=NH^+ couplings (<10 Hz) in the series. The dipositive cations Zn^{2+}, Ca^{2+}, Cd^{2+} and Pb^{2+}, as expected, constitute an intermediate case, where the chemical shift is less than 14 ppm and the CH=NH^+ coupling in the range 13.4–14.1 Hz. In accordance with the higher charge

density of the smallest tripositive cations, which presumably represent the strongest competition for O^- in the series, the weakest hydrogen bond with the smallest chemical shift and likewise the largest CH=NH^+ coupling appears in $[Sc(III)L^1]^{3+}$. These parameters reflect the position of the proton along the $N\cdots O^-$ H-bond axis. The relatively weak H-bonding in the thallic cryptate, **1**, thus suggests efficient electrostatic interaction of Tl(III) with the phenolate-O donors, in contrast to the lack of covalency in the Tl–O^- bond mentioned above.

The solubility of **1** is insufficient for solution ^{203,205}Tl or ^{13}C spectra, but ^{13}C and ^{15}N MAS-CP spectra have been obtained. These are understandably complex, given the asymmetry which differentiates the two ends of the host, the disorder which allows two different sites for the thallium(III) cation and the additional possibility of appreciable coupling to ^{203,205}Tl. In the ^{13}C spectrum, the dipolar dephasing experiment allows recognition of the methyl resonance as a relatively sharp signal near 20 ppm, and assists assignment of a broad and complex resonance in the 50–60 ppm region to methylene carbons from both ends of the crypt. The dipolar dephasing experiment also shows that the aromatic carbon signals fall into two separate ranges: 117–130 ppm for the substituted C[C]carbons and *ca*. 144 and 149 ppm for the C[H] resonances. The imino-carbon signals are assigned to a broad pair of resonances in the range 171–176 ppm, whose complexity presumably derives from the solid state disorder (between the Tl-end and protonated-end environments) as well as from ^{203,205}Tl,^{13}C coupling. Overlapped with these imino-C signals, the *ipso*-carbon resonance of the phenolate can be seen (close to 170 ppm in CD_3CN solution in these systems),[13,14] appearing strongly in the non-proton-bearing ^{13}C spectrum at 173.5 ppm.

The relative simplicity of the ^{15}N MAS-CP spectrum reflects the equivalence of the N atoms in each of the three strands of the cryptate, although the two ends are differentiated. Thus the bridgehead nitrogens present as two resonances in the normal region for N_{bridge} in these cryptates,[12] the first sharp, the second broad, at −349 and −356 ppm from the NH_4NO_3 standard, respectively, suggesting minimal coordination interaction at the Tl end. The protonated imino-nitrogen resonance appears close to −201 ppm and the Tl-coordinated imino nitrogen as a pair of resonances centred on −116 ppm with a large $^1J(^{203,205}Tl,^{15}N)$ coupling of 1002 Hz. The ^{35}Cl resonance is sharp and unsplit, near 1000 ppm, demonstrating the completely ionic character of the counterion.

The large coupling constants of ligand protons and donor-nitrogens to encapsulated ^{203,205}Tl(III) in **1** presumably derives from covalency in the Tl–N bond. The relatively weak $NH^+\cdots O^-$ hydrogen bond for **1** in turn testifies to a strong, though mainly electrostatic, interaction between Tl(III) and phenolate O^-. This suggests the probability of good complexation thermodynamics for thallium in these aminophenolate hosts, which, allied to the demonstrated kinetic stabilisation against decomplexation, indicates application as sequestering agents, at least under abiological conditions. Complexation studies are thus planned.[15]

Experimental

Synthesis of cryptates

$[TlL^1](ClO_4)_3$ 1. A solution of tris(2-aminoethyl)amine (0.002 mol, 0.292 g) in 30 cm^3 ethanol was added dropwise at room temperature to a stirred filtered mixture of sodium perchlorate (0.003 mol, 0.369 g) and 2,6-diformyl-4-methylphenol (0.003 mol, 0.50 g) in acetonitrile–ethanol (1 : 1 ratio, 50 cm^3). Solid thallium(III) nitrate (0.001 mol, 0.44 g) was added and the suspension stirred overnight, after which the bright yellow product was isolated. Analysis found (calculated): C, 40.03 (39.71); H, 4.48 (4.10); N, 10.00 (9.45)%. FAB-MS *m*/*z* (% abundance): 1079 $[TlL^1ClO_4]_2$ (6); 979 $[TlL^1ClO_4]$ (12); 879 $[TlL^1]$ (80).

$[ML^1](ClO_4)_n$: M = Na,[13] *n* = 1, 2; M = Ca,[14] *n* = 2, 3; M = Cd,[5] *n* = 2, 4; M = Zn,[14] *n* = 2, 6; M = In,[13] *n* = 3, 7; M = Bi,[13] *n* = 3, 8. $NaClO_4$ (0.018 mol, 2.57 g) in 50 cm^3 MeCN was added to a solution of 0.018 mol, 3.0 g 2,6-diformyl-4-methylphenol in 100 cm^3 ethanol in an ice bath over a period of 2 h. The solution was cooled and added dropwise with stirring to a stirred solution of tris(2-aminoethyl)amine (0.012 mol, 1.78 g in 150 cm^3 EtOH) over a period of 2 h. The volume of solvent was reduced to one third until separation of a microcrystalline yellow product, which was isolated in about 60% yield.

This sodium salt was the starting material in synthesis of the other cryptates **3**–**8**. 0.63 mmol, 0.58 g **2** was dissolved in 30 cm^3 MeCN and 1.25 mmol of the appropriate metal acetate dissolved in 50 cm^3 methanol was added quickly to avoid precipitation of the metal hydroxide. After 3 h stirring at rt, 2.5 mmol, 0.26 g $LiClO_4$ in 10 cm^3 MeOH was added. The solution was reduced to one third in volume, an equal volume of ethanol was added and the solvent was allowed to evaporate slowly in air, yielding the desired product in 30–50% yield.

Analysis found (calculated): **2**·$3H_2O$: C, 54.47 (54.90); H, 6.28 (6.30); N, 12.69 (13.11): **3**·$2H_2O$: C, 49.42 (49.21); H, 5.33 (5.47); N, 11.86 (11.78): **6**·2EtOH: C, 44.88 (44.81); H, 5.27 (5.21); N, 9.71 (9.73): **7**·H_2O: C, 41.78 (42.25); H, 4.46 (4.51); N, 10.05 (10.11): **8**·$4H_2O$: C, 37.01 (37.28); H, 4.84 (4.46); N, 8.72 (8.92)%.

$[ML^2](ClO_4)_n$: M = Na,[13] *n* = 1, 9; M = Y,[13] *n* = 3, 10; M = In,[13] *n* = 3, 11; M = Sc,[13] *n* = 3, 12. The sodium salt was first prepared by a slightly modified method to that described above:

$NaClO_4$ (1.8 mmol, 0.22 g) dissolved in 50 cm^3 CH_3CN was added to an ethanolic solution of 2,6 diformyl-4-tert-butylphenol (2.4 mmol, 0.40 g in 50 cm^3 EtOH) which then was added dropwise to a stirred solution of tris(2-aminoethyl)amine (1.6 mmol, 0.24 g). The yellow solution was filtered after 1 h at rt and crystallization started to occur when the volume was reduced to around one third. Cubic crystals were obtained in 57% yield. This product was used, as in the procedure described above for the L^1 cryptates, to generate the M(III) cryptates **10**–**12** in 50–75% yield. Analysis found (calculated): **9**·MeCN: C, 61.82 (62.14); H, 6.84 (7.15); N, 12.98 (13.05): **10**·3MeOH·$5H_2O$: C, 42.13 (41.79); H, 5.84 (6.00); N, 7.65 (7.65): **11**·$6H_2O$: C, 43.30 (43.52); H, 5.54 (5.89); N, 8.54 (8.46): **12**·$3H_2O$: C, 48.31 (48.02); H, 5.91 (6.00); N, 7.65 (7.65)%.

X-Ray experimental and crystal data

$C_{41}H_{50}Cl_3N_9O_{16}Tl$, **1**: $M = 1235.62$, triclinic, spacegroup $P\bar{1}$, $a = 12.072(14)$, $b = 13.025(17)$, $c = 17.76(2)$ Å, $\alpha = 89.35(1)$, $\beta = 72.94(1)$, $\gamma = 70.98(1)°$, $U = 2515$ Å^3, $Z = 2$, $D_m = 1.633$ Mg m^{-3}, $\mu = 3.448$ mm^{-1}, $F(000) = 1238.7935$ independent reflections measured on a Marresearch Image plate with Mo-Kα radiation ($\lambda = 0.71073$ Å). 95 frames were collected each with a counting time of 5 min with the plate 70 mm from the crystal. Data analysis was carried out with the XDS program.[16] The structure was solved using direct methods with the SHELX86 program[17] There were two alternate positions for the metal atom and these were refined with common thermal parameters and occupancy factors of x and $1 - x$; x refining to 0.59(1). The non-hydrogen atoms were refined with anisotropic thermal parameters. The hydrogen atoms were included in geometric positions and given thermal parameters equivalent to 1.2 times those of the atom to which they were attached. An empirical absorption correction was carried out using the DIFABS program.[18] The structure was refined on F^2 using SHELXL[19] to $R1$ 0.0782 and $wR2$ 0.1962 for the 5785 observed data with $I > 2\sigma(I)$.

CCDC reference number 186/1879.

See http://www.rsc.org/suppdata/dt/b0/b000736f/ for crystallographic files in .cif format.

Acknowledgements

We thank the EPSRC for access to services: high field NMR at Warwick, FAB-MS at Swansea, solid-state NMR at Durham, as well as for funds for the Reading University Image Plate system. OURC and QUB are thanked for support to G. M. and N. M. We are grateful to Mr A. Johans for assistance with crystallography.

References

1 P. R. Bradley-Moore, E. Lebowitz, M. W. Greene, H. L. Atkins and A. N. Ansari, *J. Nucl. Med.*, 1975, **16**, 156; J. D. Thomas, B. P. Griffin and R. D. White, *Cleveland Clin. J. Med.*, 1996, 213, and references contained therein.
2 Z. Ozcan, Z. Burak, C. Ozcan, G. Basdemir, T. Ozcar, S. Erdem and Y. Duman, *Nucl. Med. Commun.*, 1996, **17**, 805.
3 S. Galvan-Arzate and A Santamaria, *Toxicol. Lett.*, 1998, **99**, 1.
4 J.-M. Lehn and J.-P. Sauvage, *J. Am. Chem. Soc.*, 1975, **97**, 67000.
5 M. G. B. Drew, O. W. Howarth, G. G. Morgan and J. Nelson, *J. Chem. Soc.*, *Dalton Trans.*, 1994, 3149.
6 Y. Y. Lu, J. Y. Tung, J. H. Chen, F. L. Liao, S. L. Wang, S. S. Wang and L. P. Hwang, *Polyhedron*, 1998, **18**, 145.
7 Y. H. Sheu, T. N. Hong, C. C. Lin, J. H. Chen and S. S. Wang, *Polyhedron*, 1997, **16**, 681.
8 K. Schweiger, H. Huckstadt and H. Homborg, *Z. Anorg. Allg. Chem.*, 1998, **634**, 167.
9 M. G. B. Drew, O. W. Howarth, C. J. Harding, N. Martin and J. Nelson, *J. Chem. Soc.*, *Chem. Commun.*, 1995, 903.
10 A. J. Amoroso, J. C. Jeffrey, P. L. Jones, J. A. McCleverty, E. Psillakis and M. D. Ward, *J. Chem. Soc.*, *Chem Commun.*, 1995, 1175; G. Ferguson, M. C. Jennings, F. J. Lalor and C. Shanahan, *Acta Crystallogr.*, *Sect. C*, 1991, **47**, 2079; A. H. Cowley, R. L. Geerts, C. M. Nunn and S. Trot, *J. Organomet. Chem.*, 1989, **365**, 19.
11 O. W. Howarth, V. McKee and J. Nelson, *Chem. Commun.*, 2000, 21.
12 D. C. Apperley, W. Clegg, S. Coles, J. L. Coyle, N. Martin, B. Maubert, V. McKee and J. Nelson, *J. Chem. Soc.*, *Dalton Trans.*, 1999, 229.
13 N. Martin, Ph.D., Queens University Belfast, 1996.
14 G. G. Morgan, Ph.D., Open University, 1995.
15 F. Arnaud-Neu, R. M. Town and J. Nelson, work in progress.
16 W. Kabsch, *J. Appl. Crystallogr.*, 1988, **21**, 916.
17 G. M. Sheldrick, *Acta Crystallogr.*, *Sect. A*, 1990, **46**, 467.
18 N. Walker and D. Stuart, *Acta Crystallogr.*, *Sect. A*, 1983, **39**, 158.
19 G. M. Sheldrick, SHELXL, Program for crystal structure refinement, University of Göttingen, 1993.